Eur. Phys. J. D **37**, 163–169 (2006)
DOI: 10.1140/epjd/e2005-00276-4

THE EUROPEAN PHYSICAL JOURNAL D

Stark broadening and shift measurements of two doubly excited NI multiplets

A. Bartecka, A. Bacławski[a], T. Wujec, and J. Musielok

Institute of Physics, Opole University, ul. Oleska 48, 45-052 Opole, Poland

Received 9 June 2005 / Received in final form 16 September 2005
Published online 11 October 2005 –

Abstract. Experimental Stark-broadening studies of two selected doubly excited NI multiplets from the infrared wavelength range are presented. One of them is very sensitive to interactions with charged particles in plasmas and the other exhibits — at the same plasma conditions — only very small broadening and shift. A high current wall-stabilized arc operated in helium with admixture of nitrogen and hydrogen was applied as the excitation source. The radiation of the plasma was detected by applying a grating spectrometer equipped with a CCD detector. Measurements were performed at electron densities of the plasma between 3×10^{15} and 7×10^{15} cm^{-3}, corresponding to temperatures from the range 8000–10500 K. Electron impact widths (w_e) and shifts (d_e) of fine structure components of these multiplets were determined. The evaluated Stark broadening parameters (w_e, d_e) are compared with other experimental data and with calculated Stark effect constants.

PACS. 32.70.Jz Line shapes, widths, and shifts – 52.70.Kz Optical (ultraviolet, visible, infrared) measurements

1 Introduction

Recently performed emission measurements utilizing high current wall-stabilized arcs provided new spectroscopic data concerning e.g. the NI spectrum [1–5]. Among these data especially interesting appear the line strengths and Stark broadening parameters for a few doubly excited NI multiplets. Two recent works performed in our laboratory were devoted to studies of the broadening of one of these transitions, namely the $(^1\mathrm{D})3s\ ^2\mathrm{D} - (^1\mathrm{D})3p\ ^2\mathrm{P}^o$ multiplet [4,5]. (In further parts of the paper we use the shorter notation $3s' - 3p'$ instead of $(^1\mathrm{D})3s - (^1\mathrm{D})3p$). The fine structure components of this transition reveal significant red shift and large broadening. On the other hand, preliminary investigations performed by Musielok [6] show, that the broadening and shift parameters of two other multiplets (members of the same transition array $3s' - 3p'$), differ from each other as well from that studied in [4,5]. The fine structure components of one of these multiplets ($3s'\ ^2\mathrm{D} - 3p'\ ^2\mathrm{F}^o$) appear as very narrow spectral features and show negligible shifts, while the components of the other one ($3s'\ ^2\mathrm{D} - 3p'\ ^2\mathrm{D}^o$) exhibit large broadening and significant blue shifts, i.e. in the opposite direction than has been found in the case of the $3s'\ ^2\mathrm{D} - 3p'\ ^2\mathrm{P}^o$ multiplet studied in [4,5]. Unfortunately Stark broadening calculations for lines originating from this transition array ($3s' - 3p'$) are not available in literature.

Comparison of recent line strengths calculations [7–10] for this particular transition array shows good agreement in the case of the multiplet revealing very weak broadening and shift, but large discrepancies in the case of the two significantly broadened and shifted multiplets. In the case of the transitions $3s'\ ^2\mathrm{D} - 3p'\ ^2\mathrm{P}^o$ and $3s'\ ^2\mathrm{D} - 3p'\ ^2\mathrm{D}^o$, the CIV3 data of Hibbert et al. [7–9] are exceeding those calculated by the Opacity team [10] by a factor of 1.55 and 1.84, respectively. Experimental tests performed by measuring intensity ratios of selected multiplets indicate that in the case of the above mentioned transitions the Opacity calculations seem to provide more reliable data [2].

Our present paper is devoted to studies of two NI multiplets: $3s'\ ^2\mathrm{D} - 3p'\ ^2\mathrm{D}^o$ and $3s'\ ^2\mathrm{D} - 3p'\ ^2\mathrm{F}^o$, showing significantly different broadening and shift due to the Stark effect in plasmas.

2 Experiment

2.1 Plasma source and experimental method

A high current wall-stabilized arc running in helium with small admixtures of nitrogen and hydrogen (4.5% and 0.5% by volume respectively) was applied as the excitation source of the studied spectra. The stabilizing wall, consisting of several copper plates isolated from each other, forms a discharge channel of a length of 70 mm. At both ends of this channel two electrodes were mounted: a tungsten rod and a copper ring, serving as cathode and anode, respectively. The concentration of nitrogen in the plasma was kept at a rather small level in order to avoid possible self-absorption of NI line radiation along the arc axis.

[a] e-mail: abac@uni.opole.pl

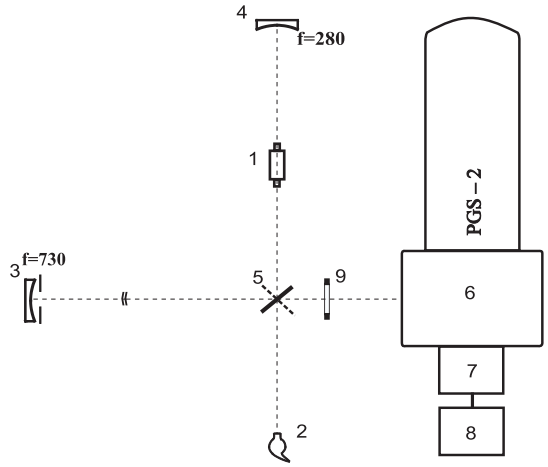

Fig. 1. The scheme of the experimental set-up is shown. The numbers denote: 1 and 2 — the wall-stabilized arc and the radiometric standard source; 3 and 4 — concave mirrors; 5 — rotational flat mirror; 6 — spectrometer; 7 — OMA4 detector; 8 — computer; 9 - edge spectral filter.

The areas close to the electrodes (regions of lower temperature) were additionally supplied with some amount of argon, e.g. in order to improve the stability of the discharge. Since our measurements were performed in end-on direction, the presence of argon in the vicinity of electrodes reduces also significantly the contribution of NI and H radiation from these cooler plasma layers as well as assures optically thin conditions for radiation originating from the central (high-temperature) region of the arc column. The arc which is described in details e.g. in [11,12] was operated at atmospheric pressure at five arc currents, ranging from 29 to 50 A in order to obtain different plasma parameters: electron densities and temperatures. Measurements were performed by applying the spectrometer PGS-2 equipped with a reflection grating with 1300 grooves/mm blazed at 550 nm. The radiation was detected applying a two-dimensional Optical Multichannel Analyzer (OMA 4), with regular pixel gaps of 0.019 mm, mounted in the exit focal plane of the spectrometer. This instrumentation provides spectra with a reciprocal dispersion from 5.6 to 6.7 pm/pixel, depending on the studied wavelength range.

Figure 1 shows schematically our experimental set-up. The radiation originating either from the arc (1) or from the tungsten standard lamp (2) was imaged via the flat rotational mirror (5) and the concave mirror (3) onto the 20 μm wide entrance slit of the spectrometer. The large focal length of the mirror (3) ($f = 730$ mm) and the use of the diaphragm ($\Phi = 12$ mm), placed in front of the concave mirror, restrict the collection angle for the light emitted from the arc column and thus allow selecting radiation originating from plasma layers parallel to the arc axis. This optical imaging system assures that radiation emitted from well-defined nearly homogeneous plasma volumes could be measured. The homogeneity of individual selected plasma layers was checked by measuring the ratio between the peak separation and the $FWHM$ of the H_β line (see Sect. 2.2). The concave mirror (4) was applied for checking optically thin conditions of plasma layers parallel to the arc axis. That concave mirror forms an arc image in its own volume and thus nearly doubles the measured intensities. Comparison of spectral line distributions determined with and without back-reflection of light yields reliable information about (possible) self-absorption of radiation in the plasma. If the ratio between signals measured with and without back reflection remains constant over the whole line profile the assumption of optical thin conditions is then justified. In front of the entrance slit a suitable edge filter (9) was placed in order to suppress the radiation from higher order spectra.

The OMA4 detector enables to measure simultaneously the radiation from a spectral interval of about 7 nm (in the case if the grating with 1300 grooves/mm is used). The dimension of the detector in direction perpendicular to the wavelength axis allows measuring radiation originating from the whole diameter of the arc. However, for further evaluation only those spectra have been taken which originate from plasma layers spaced from the arc axis less then 1.0 mm, i.e. from plasma volumes with weak radial gradients.

The apparatus profile was determined applying a low-pressure argon-discharge lamp of a Plücker type. At the entrance slit of the spectrometer set to 20 μm the apparatus profile has been found to be of Gaussian type with a $FWHM$ of 11 pm, i.e. less than 2 pixels. The Plücker tube ran in argon was also used as a standard source for wavelength calibration of the measured spectra.

2.2 Plasma diagnostics

For studies of Stark-broadening parameters the knowledge of the main plasma parameters — the electron density and electron temperature is indispensable. Especially important is the accurate knowledge of the electron density, because — according to theoretical considerations — the Stark widths and shifts of spectral lines (in first approximation) are proportional to the electron density. This plasma parameter (N_e) was determined from measured $FWHM$ of the hydrogen H_β line using the theoretical broadening data of Gigosos and Cardeñoso [13]. Applying different arc currents and selecting various plasma layers (spaced from the axis by different distances), spectra emitted from nearly homogeneous volumes were measured, corresponding to electron density values from 3.0×10^{15} cm^{-3} to 7.0×10^{15} cm^{-3}. The uncertainties of our electron density measurements we estimate to be less than 10%. Besides the full widths at half maximum ($FWHM$) we also measured the peak separation of H_β profiles. In this way we were able to test if the radiation originated from homogeneous plasma layers. Possible departures from homogeneity of the plasma volume should result in noticeable departure of the ratio $R = (\Delta\lambda^{peak\ sep.}/FWHM)$ from the value 0.36±0.01 [14,15]. Since we restricted our measurements to plasma layers being not too far from the arc axis (weak parameter gradients) the homogeneity requirements were well fulfilled.

The plasma temperature T_e was determined by measuring total line intensities of spectral lines and applying the standard Boltzmann plot method. The following NI spectral lines (wavelengths given in nm) were taken for this purpose: 856.774, 870.325, 871.884, 902.892, 904.588, 904.989 and 906.048. The excitation energies of these lines are in the range from 11.75 to 13.73 eV, i.e. the energy gap ($\Delta E \approx 2$ eV) is sufficient for reliable temperature determination. The corresponding transition probabilities have been taken from [16]. In this way, for different arc currents and plasma layers, temperatures in the interval 8000–10500 K have been determined. The uncertainty of the temperature determination we estimate to be about ±500 K. Assuming that the gas temperature is the same as the excitation temperature (in arc plasmas under atmospheric pressure this assumption is justified) it was possible to determine the Doppler broadening of spectral lines corresponding to the evaluated temperature interval. For the studied NI multiplets the Doppler widths (*FWHM*) do not exceed 20 pm.

3 Analysis of the spectra and data reduction

For each plasma condition (arc current, selected plasma layer) and each wavelength interval, corresponding to the studied spectra, at least three independent expositions of the OMA4 detector have been performed. Then the respective spectra (from the arc and from the standard source) were averaged and wavelength calibrated applying the spectra emitted from the Plücker tube. In further steps of data reduction these averaged and wavelength calibrated spectra were analyzed and evaluated.

The multiplet $3s'\ ^2\mathrm{D} - 3p'\ ^2\mathrm{D}^o$ consists of four fine structure components at the following (non-shifted) wavelengths: 918.745, 918.786, 920.759 and 920.800 nm, which correspond to transitions between levels with the following (lower-upper) J-values: 5/2–5/2, 3/2–5/2, 5/2–3/2, 3/2–3/2, respectively. The corresponding transition probabilities (A_{ki}) for individual spectral lines have been taken from [16]. Using these A_{ki} values and the temperatures of our experiments the respective line intensity fractions of: 0.540, 0.039, 0.060 and 0.361 have been obtained. Because of the small differences in wavelengths ($\Delta\lambda = 41$pm) between spectral lines originating from the same upper level, this multiplet appears — at our plasma conditions and spectral resolution — in form of two spectral features, both consisting of two fine structure components.

The second studied multiplet $3s'\ ^2\mathrm{D} - 3p'\ ^2\mathrm{F}^o$ consists of three fine structure components at wavelengths: 904.588, 904.949 and 904.989 nm, corresponding to transition between levels 5/2–7/2, 5/2–5/2 and 3/2–5/2, respectively. The first (strongest) transition is well isolated, but the two others — originating from the upper level 5/2 — overlap and appear like a single spectral line. According to the LS coupling scheme the relative intensities of these three components at temperatures of our experiments are 0.501, 0.034, 0.465, respectively.

In Figure 2a we present an example of the measured NI spectrum together with the corresponding reference signal

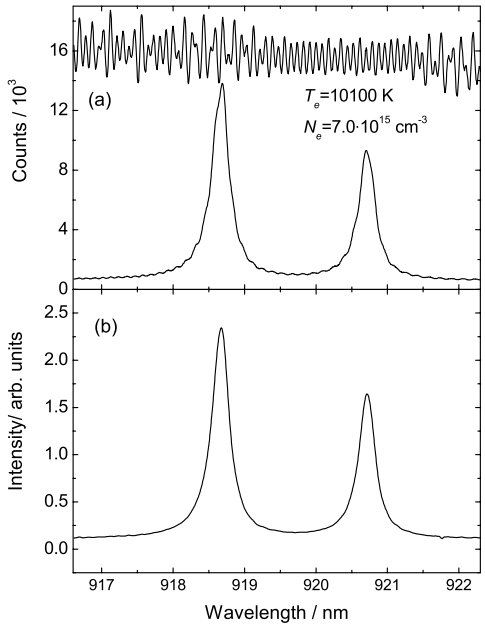

Fig. 2. An example of our registration of the NI $3s'\ ^2\mathrm{D} - 3p'\ ^2\mathrm{D}^o$ multiplet, illustrating the reduction of experimental data: (a) the directly measured spectra from the arc and the radiometric standard source, (b) the NI spectrum calibrated against the standard source signal and after applying the smoothing procedure (Fourier transform technique).

from the tungsten strip standard source in the wavelength range from 916.6 to 922.3 nm, i.e. comprising the emission from the multiplet $3s'\ ^2\mathrm{D} - 3p'\ ^2\mathrm{D}^o$. Both, the studied NI multiplet and the standard source spectrum are superimposed by a significant interference pattern. The amplitude of this pattern has been found to be proportional to the light intensity. In order to release the measured signals from this disturbing interference pattern the directly recorded spectra were filtered applying the Fourier transform technique described in [5,11]. As can be seen in Figure 2b, the smoothing procedure removes the regular interference pattern, yielding reliable NI line shapes. However, the Fourier transform technique may distort significantly the shape of narrow spectral lines, i.e. having widths comparable to the widths of interference peaks. Therefore this technique was applied only for the strongly broadened NI multiplet and the analysis of the hydrogen H_β line, but was not applied for the evaluation of the narrow $3s'\ ^2\mathrm{D} - 3p'\ ^2\mathrm{F}^o$ transition.

After applying the smoothing procedure the measured spectra were calibrated against the corresponding light outputs of the standard source. The results obtained at four different plasma conditions (different N_e and T) for the NI transition $3s'\ ^2\mathrm{D} - 3p'\ ^2\mathrm{D}^o$, after applying the smoothing procedure and after calibration against the signal from the tungsten strip lamp, are shown in Figure 3. As can be seen the lines are significantly broadened, revealing some asymmetry and exhibiting large blue shifts which increase with growing electron density.

In Figure 4 similar results obtained for the $3s'\ ^2\mathrm{D} - 3p'\ ^2\mathrm{F}^o$ multiplet (without applying the smoothing

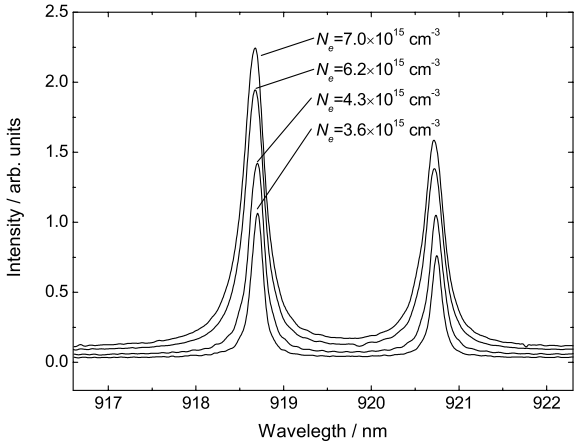

Fig. 3. The spectra of the NI $3s'\ ^2\mathrm{D}-3p'\ ^2\mathrm{D}^o$ transition at four different electron densities and plasma temperatures, after applying the smoothing procedure and after intensity calibration against the standard source.

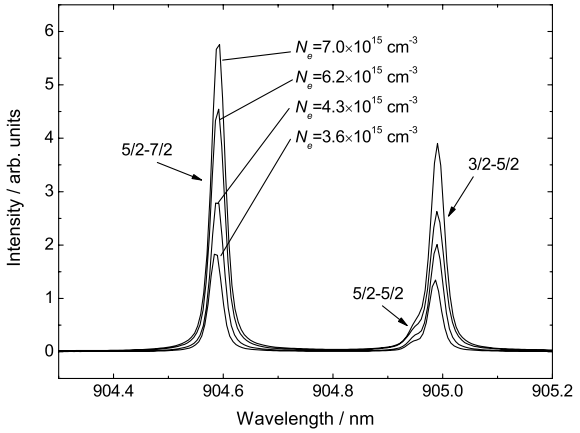

Fig. 4. The spectra of the NI $3s'\ ^2\mathrm{D}-3p'\ ^2\mathrm{F}^o$ multiplet recorded at four different electron densities and plasma temperatures after intensity calibration against the standard source (without applying the smoothing procedure).

procedure), are shown. The Stark widths of the single fine structure component at 904.588 nm are systematically about 13 times narrower than the corresponding widths of the stronger spectral features around $\lambda = 918.7$ shown in Figure 3. Nevertheless one may infer that the broadening is somewhat growing with increasing electron density. At our plasma conditions accurate studies of Stark broadening and shift of this transition as a function of electron density are difficult, because the contribution from Doppler broadening is comparable to the Stark effect and because of the too small resolution of our spectral instrumentation.

4 Theoretical background and the fitting procedure

Spectral lines of neutral atoms emitted from plasmas are usually affected by a few broadening mechanisms. In most cases the measured spectral line shapes can be regarded as a convolution of profiles resulting from these various broadening effects. In the case of non-hydrogenic transitions (single fine structure components) the main contribution arises from collisions between emitters and fast moving electrons, producing shifted Lorentzian-like line shapes. Collisions with ions lead to some (usually small) additional broadening and cause an asymmetry of the profile enhancing that line wing, which corresponds to the shift direction. Such profiles which include the ion broadening can be described by an asymmetric function introduced by Griem [17]. Since at our plasma conditions the Stark broadening and shift caused by electron collisions is the dominant mechanism we have decided to use symmetrical line shapes for matching our experimental data and to study the asymmetry by analyzing the discrepancies between fitted symmetrical functions and the measured profiles.

Other broadening mechanisms contributing to the measured line profiles at plasma conditions of our experiments are the Doppler and instrumental broadening. If the gas temperature T is known, the Doppler full width at half maximum ($FWHM$) can easily be calculated from the relation:

$$\Delta\lambda_{1/2}^{D} = \frac{2\lambda_l^0}{c}\sqrt{\frac{2kT\ln 2}{m}}, \tag{1}$$

where λ_l^0 is the wavelength of the unperturbed line and m is the mass of the emitting atom. As mentioned earlier the instrumental width $\Delta\lambda_{1/2}^{i}$ was measured using a low-pressure discharge lamp. The shape of this instrumental profile could be well approximated with a Gaussian function. The convolution of this Gaussian function and the Doppler profile leads obviously also to a Gaussian function with the $FWHM$ given by:

$$\Delta\lambda_{1/2}^{G} = \sqrt{(\Delta\lambda_{1/2}^{D})^2 + (\Delta\lambda_{1/2}^{i})^2}. \tag{2}$$

The convolution of this resultant Gaussian profile with the Lorentzian shape, produced by collisions of emitters with electrons, leads to a symmetrical Voigt profile describing the shape of a single fine structure component (l):

$$V(\lambda) = I_l \frac{2\ln 2}{\pi^{3/2}} \frac{w_{1/2}^{L}}{w_{1/2}^{G}} \times \int_{-\infty}^{+\infty} \frac{\exp(-\lambda'^2)d\lambda'}{\left(\sqrt{\ln 2}\frac{w_{1/2}^{L}}{w_{1/2}^{G}}\right)^2 + \left(\sqrt{4\ln 2\frac{\lambda-\lambda_l}{w_{1/2}^{G}} - \lambda'}\right)^2}, \tag{3}$$

where $w_{1/2}^{L}$ is the Lorentzian $FWHM$, while λ_l and I_l are the wavelength position and the intensity of the measured (shifted) line peak, respectively.

We have assumed that within a given multiplet the Stark broadening parameters: the electron widths $w_e = w_{1/2}^{L}/2$ and the electron shifts $d_e = (\lambda_l - \lambda_l^0)$ are the same for each fine structure component (line). The Gaussian contribution ($\Delta\lambda_{1/2}^{G}$) to the Voigt profile, which includes

the instrumental and Doppler broadening, has been taken from equation (2), assuming that the gas temperature is equal to the electron temperature obtained from the Boltzmann plot method. The wavelengths of non-shifted individual fine structure components (λ_l^0) and the respective transition probabilities have been taken from [16]. As mentioned in Section 3 from these transition probability values the relative intensities (I_l) of individual fine structure components within the given multiplet have been computed and their sum was normalized to the value of one. The experimental data were finally fitted according to the following formula:

$$P(\lambda) = a\lambda + b + I_0 \sum_l V_l(\lambda), \qquad (4)$$

and the summation was spread out over all fine structure components (l) of the multiplet. The fitting parameters are the Lorentzian $FWHM$ $w_{1/2}^L$, the shift in wavelength, obeying the relation $d_e = (\lambda_l - \lambda_l^0)$ for each fine structure component (l), the intensity factor I_0, and two parameters (a, b) for the description of the continuum background radiation $I_{cont} = a\lambda + b$.

Since we have used symmetrical profiles in our fitting procedure, we focused our attention on accurate matching of line wings being opposite to the shift direction. The differences between intensities of the measured spectra and the fitted ones we interpret as the result of ion broadening, which produces line asymmetries and consequently enhances the line wings corresponding to the shift direction.

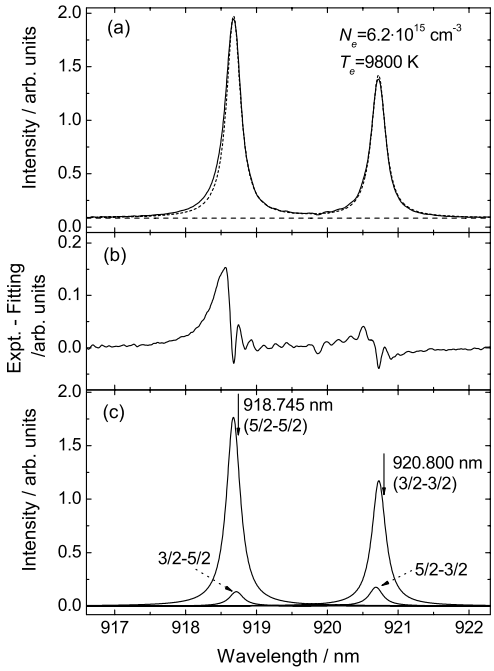

Fig. 5. An example of the analysis of a measured spectrum (multiplet $3s'\ ^2\mathrm{D} - 3p'\ ^2\mathrm{D}^o$) illustrating the fitting procedure: (a) comparison of measured (solid line) and fitted (short-dashed line) spectrum; the dashed line represents the background continuum, (b) the difference between the measured spectral intensity distribution and the fitted spectrum (intensity scale expanded 5 times), (c) the fitted profiles decomposed into fine structure components.

5 Results and discussion

Applying the fitting procedure we were able to determine — for each plasma condition — the electron impact widths w_e and shifts d_e for the single fine structure component of the multiplet. As an example of our measurements we present in Figure 5a the measured spectrum (solid line) and the fitting results (short dashed line) for the multiplet $3s'\ ^2\mathrm{D}-3p'\ ^2\mathrm{D}^o$ at $N_e = 6.2\times10^{15}$ cm^{-3} and $T = 9800$ K. The dashed line represents the background continuum. In Figure 5b, the difference between the experimental shape and the fitted one is shown in an intensity scale expanded about 5 times, while in Figure 5c, the shapes of all fine structure components resulting from the fitting procedure are presented. The vertical arrows in Figure 5c show the wavelength positions of the two stronger unperturbed lines within each line pair. From Figure 5a, it can be seen that the multiplet exhibits an asymmetry enhancing the blue wings of the components. Since we used Voigt profiles in our fitting procedure, the difference presented in Figure 5b can be regarded as a measure of the line asymmetry, which has not been included in our fitting procedure. As can be seen the asymmetry is more evident in the case of the stronger line pair around 918.75 nm. This is caused by the "true" asymmetry of the stronger component (5/2–5/2) but also by the influence of the weaker component (3/2–5/2) positioned slightly towards longer wavelengths. In the case of the line pair around 920.8 nm, the weaker component appears on the blue wing of the stronger one and thus leading to the less apparent asymmetry.

The electron impact widths w_e determined for the second studied multiplet ($3s'\ ^2\mathrm{D}-3p'\ ^2\mathrm{F}^o$) are in the average about 13 times smaller than for the transition $3s'\ ^2\mathrm{D}-3p'\ ^2\mathrm{D}^o$. The uncertainties of w_e determination in the case of this narrow transition are significantly larger, because at our plasma conditions the Stark broadening is of the same order of magnitude as the instrumental and Doppler broadening. Therefore the results obtained for this multiplet can be regarded as giving only an estimation of electron impact Stark widths. Even more critical are our shift measurements for this weakly broadened transition. The only reliable statement which can be given regarding this Stark broadening parameter is that the multiplet is — at our plasma conditions — probably somewhat red shifted by a value not exceeding one pixel of our detector, i.e. less than 6 pm.

According to theoretical considerations both electron impact parameters (w_e and d_e) are linear functions of the electron density in the plasma. Therefore the ratio of these two broadening parameters should depend only on the plasma temperature. In Figure 6 we plot the ratios d_e/w_e versus the temperature of the plasma. The uncertainty limits of our measurements do not allow making

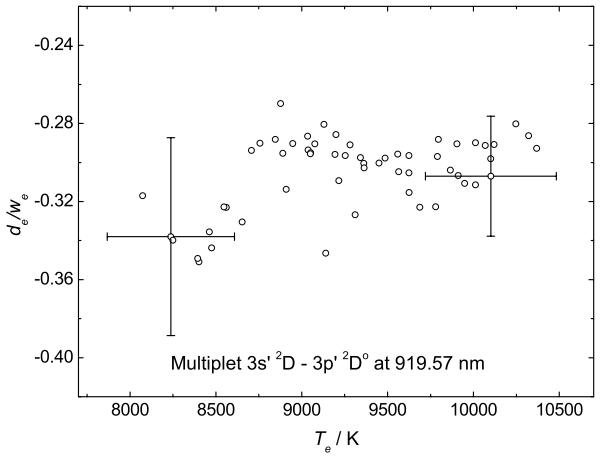

Fig. 6. The shift to width ratios, d_e/w_e, determined for lines belonging to the $3s'\ ^2\mathrm{D} - 3p'\ ^2\mathrm{D}^o$ multiplet versus the temperature of the plasma.

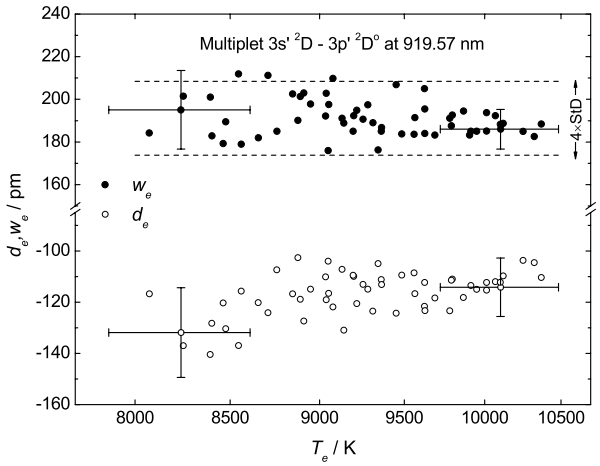

Fig. 7. The electron impact widths (w_e) and shifts (d_e) determined for fine structure components of the multiplet $3s'\ ^2\mathrm{D} - 3p'\ ^2\mathrm{D}^o$, normalized to the standard electron density of $10^{16}\mathrm{cm}^{-3}$ plotted as a function of the temperature of the plasma.

reliable conclusions about a possible dependence of this ratio in the temperature range of our experiments (8000–10500 K).

The electron impact widths and shifts determined for the multiplet $3s'\ ^2\mathrm{D} - 3p'\ ^2\mathrm{D}^o$ at different electron densities have been normalized to the standard electron density value of 10^{16} cm^{-3} [17]. In Figure 7 these normalized electron impact widths (w_e) and shifts (d_e) are shown as a function of the plasma temperature. As can be seen, again no clear temperature dependence could be found. Somewhat smaller shifts are found at temperatures below 8500 K. However, this observation has to be regarded as being questionable because the uncertainties of our shift and widths measurements at lower temperatures are significantly larger than for higher temperatures, as shown in the figure by the corresponding error bars. The error bars of the determined electron impact widths and shifts shown in Figures 6 and 7 arise from the following main sources: (i) the systematic error originating from fitting symmetrical Voigt profiles to shapes exhibiting small asymmetry (3–5%); (ii) the uncertainty of the applied fitting procedure, estimated to be in the range from 4 to 6%; and (iii) the uncertainties of the determination of the electron density of the plasma (8–10%).

6 Calculations of Stark effect constants and comparison with measured broadening parameters

As mentioned earlier the main broadening mechanism in the case of the studied NI transitions at our plasma conditions is the quadratic Stark effect. Since the observed widths and shifts of the studied spectral lines differ significantly we decided to compare these broadening parameters with the primary Stark broadening quantity, namely the Stark effect constants. In the case of non-hydrogenic emitters the Stark effect constant is given by [18,19]:

$$C_4 = C_{4,i} - C_{4,f}, \tag{5}$$

where i and f denote the initial and final energy level, respectively. The parameter $C_{4,i}$ is given by:

$$C_{4,i} = \frac{e^2}{3\hbar^2 g_i} \sum_j \frac{S_{ij}}{\omega_{ij}} = \frac{e^2}{3\hbar g_i} \sum_j \frac{S_{ij}}{E_i - E_j}, \tag{6}$$

and the summation has to be executed over all levels j (E_j) in the neighbourhood of level i (E_i), for which optical transitions exist. S_{ij}, ω_{ij} and g_i are the line strengths, angular frequencies for involved transitions and the statistical weight of upper level respectively. An analogous formula holds for $C_{4,f}$. The line strengths S_{ij} and the excitation energies E_i and E_j have been taken from the NIST database available in Internet [20]. Calculations were performed for transitions studied in this work, reported in our previous paper [5] and — for comparison purposes — for some selected NI lines studied by Jones et al. [21] and Helbig et al. [22]. Since the Stark effect constants for individual lines belonging to a given multiplet differ only insignificantly, we quote in Table 1 only the mean C_4 value characterizing the whole multiplet. Because the line shift is proportional to the Stark effect constant ($\Delta\omega \sim C_4$), the sign of C_4 determines the direction of the line shift: blue shifts occur for $C_4 > 0$, and red shifts are observed for $C_4 < 0$. The main broadening parameter γ may by calculated knowing the plasma conditions (N_e and T) from the formula [18]:

$$\gamma = 9.7 \times 10^2\ C_4^{2/3}\ N_e\ T^{1/6} \left(1 + \frac{2m_e}{m}\right)^{1/6}, \tag{7}$$

where m_e and m are the electron and emitter mass, respectively. In the last two columns of Table 1 the normalized broadening and shift parameters (w_e and d_e) quoted in frequency units obtained in this work, determined in our previous paper [5], and taken from other experimental papers [21,22] are listed.

Table 1. Comparison of computed Stark effect constants C_4 and the resulting broadening parameters γ with measured (normalized to the standard electron density value of 10^{16} cm^{-3}) electron impact widths w_e and shifts d_e quoted in frequency units.

Transition	$C_4 \times 10^{13}$ (cm^{4}s^{-1})	γ (GHz)	w_e (GHz)	d_e (GHz)
$3s'\ ^2\mathrm{D} - 3p'\ ^2\mathrm{P}^o$	–8.94	66.5	61[a]	48[a]
$3s'\ ^2\mathrm{D} - 3p'\ ^2\mathrm{F}^o$	0.000316	0.07	5.3	1.5
$3s'\ ^2\mathrm{D} - 3p'\ ^2\mathrm{D}^o$	17.1	102	68	–41
$3s\ ^2\mathrm{P} - 3p'\ ^2\mathrm{D}^o$	17.1	102	66[b]	
			64[c]	–25[c]
$3s\ ^2\mathrm{P} - 4p\ ^2\mathrm{S}^o$	0.585	10.8	13[b]	
			13[c]	–3.7[c]
$3s\ ^4\mathrm{P} - 4p\ ^4\mathrm{S}^o$	-0.910	14.5	14[b]	
			13[c]	12[c]

[a] A. Bartecka et al., Eur. Phys. J. D **29**, 265 (2004).
[b] D.W. Jones et al., Phys. Rev. A **35**, 2585 (1987).
[c] V. Helbig et al., Phys. Rev. A **14**, 1082 (1976).

Our calculations explain qualitatively the observed widths and shifts of spectral lines belonging to the $3s'-3p'$ transition array studied in this work ($^2\mathrm{D}-^2\mathrm{F}^o$, $^2\mathrm{D}-^2\mathrm{D}^o$) and in our previous paper ($^2\mathrm{D}-^2\mathrm{P}^o$) [5]. Especially interesting is the computed result for the multiplet $3s'\ ^2\mathrm{D}-3p'\ ^2\mathrm{F}^o$ predicting very small line broadening and shift. Indeed lines belonging to this multiplet are found to be very narrow and consequently also the shifts are very small. Nevertheless a disagreement appears in the shift direction: calculations predict weak blue shifts, while our measurements seem to indicate small red shifts. However, since the C_4 value computed for the multiplet $3s'\ ^2\mathrm{D}-3p'\ ^2\mathrm{F}^o$ is at least 4 orders of magnitude smaller than for the two other multiplets ($^2\mathrm{D}-^2\mathrm{P}^o$ and $^2\mathrm{D}-^2\mathrm{D}^o$), the obtained C_4 value has to be regarded as being significantly less reliable.

Since the contribution to the Stark effect constants C_4 arise mainly from "interactions" of energy levels with the upper level under consideration, it is not surprising that the results determined for the multiplets $3s'\ ^2\mathrm{D}-3p'\ ^2\mathrm{D}^o$ and $3s\ ^2\mathrm{P}-3p'\ ^2\mathrm{D}^o$ are the same — 17.1×10^{-13} cm^{4}s^{-1}. Experimental data obtained by Jones et al. [21] and Helbig et al. [22], based on line profile measurements in the UV spectral range (λ = 410.69 nm, $3s\ ^2\mathrm{P}-3p'\ ^2\mathrm{D}^o$), are in very good agreement with our result for the infrared transition $3s'\ ^2\mathrm{D}-3p'\ ^2\mathrm{D}^o$. Our computed Stark effect constants for the last two multiplets listed in Table 1, are also in accordance with the corresponding widths and shifts observed in [21,22].

7 Conclusions

Stark broadening and shift parameters of two doubly excited infrared multiplets of NI, belonging to the same transition array have been determined. Both multiplets share the same lower term. One of them ($3s'\ ^2\mathrm{D}-3p'\ ^2\mathrm{D}^o$) shows very strong broadening and shift, while the second one ($3s'\ ^2\mathrm{D}-3p'\ ^2\mathrm{F}^o$) — at the same plasma conditions — appear in form of very narrow spectral lines. Calculations of Stark effect constants C_4, being the primary Stark broadening parameters for non-hydrogenic spectral lines, allow explaining qualitatively the observed differences in line broadening and shift. The electron impact width (w_e) for the broad transition (upper level $3p'\ ^2\mathrm{D}^o$) agree well with the data obtained by Jones et al. [21] and by Helbig et al. [22], while studying the multiplet $3s\ ^2\mathrm{P}-3p'\ ^2\mathrm{D}^o$ in the UV spectral range. Also the results of our previous study [5], devoted to the third member of this transition array ($3s'\ ^2\mathrm{D}-3p'\ ^2\mathrm{P}^o$), exhibiting shifts in the opposite direction than the multiplet $3s'\ ^2\mathrm{D}-3p'\ ^2\mathrm{D}^o$, are consistent with the calculated Stark effect constants.

References

1. J. Musielok, W.L. Wiese, G. Veres, Phys. Rev. A **53**, 3588 (1995)
2. J. Musielok, J.M. Bridges, J.R. Fuhr, W.L. Wiese, Phys. Rev. A **61**, 044502 (2000)
3. A. Bacławski, T. Wujec, J. Musielok, Phys. Scripta **65**, 28 (2002)
4. T. Wujec, J. Halenka, A. Jazgara, J. Musielok, J. Quant. Spectrosc. Radiat. Transfer **74**, 663 (2002)
5. A. Bartecka, T. Wujec, J. Musielok, Eur. Phys. J. D **29**, 265 (2004)
6. J. Musielok (unpublished)
7. A. Hibbert, E. Biémont, M. Godefroid, N. Vaeck, Astron. Astrophys. Suppl. Ser. **88**, 505 (1991)
8. A. Hibbert, E. Biémont, M. Godefroid, N. Vaeck, J. Phys. B **24**, 3943 (1991)
9. A. Hibbert, E. Biémont, M. Godefroid, N. Vaeck, Astron. Astrophys. Suppl. Ser. **99**, 179 (1993)
10. D. Luo, A.K. Pradhan, J. Phys. B **22**, 3377 (1989)
11. T. Wujec, W. Olchawa, J. Halenka, J. Musielok, Phys. Rev. E **66**, 066403 (2002)
12. T. Wujec, A. Bacławski, A. Golly, I. Książek, Acta Phys. Pol. A **96**, 333 (1999)
13. M.A. Gigosos, V. Cardeñoso, J. Phys. B **29**, 4795 (1996)
14. W.L. Wiese, *Proc. 7th Yugoslav Symp. & Summer School on Phys. Ionized Gases,* Dubrovnik, 637 (1974)
15. F. Torres, M.A. Gigogos, S. Mar, J. Quant. Spectrosc. Radiat. Transfer **31**, 266 (1984)
16. W.L. Wiese, J.R. Fuhr, T.M. Deters, *Atomic transition probabilities of carbon, nitrogen and oxygen: a critical data compilation* (J. Phys. Chem. Ref. Data, Monograph **7**, 1996)
17. H.R. Griem, *Spectral line broadening by plasmas* (Academic Press, New York, 1974)
18. R. Rompe and M. Steenbeck, *Progress in Plasmas and Gas Electronics* (Akademie-Verlag, Berlin, 1975), Vol. 1
19. G. Traving, Line broadening and line shift, In *Plasma diagnostics* (North Holland Publ. Co., Amsterdam, 1968)
20. *NIST Atomic Spectra Database* `http://physics.nist.gov/PhysRefData/ASD/index.html`
21. D.W. Jones, G. Pichler, W.L. Wiese, Phys. Rev. A **35**, 2585 (1987)
22. V. Helbig, D.E. Kelleher, W.L. Wiese, Phys. Rev. A **14**, 1082 (1976)